Transport Across Irregular Interfaces : Fractal Electrodes, Membranes and Catalysts

Bernard Sapoval

Laboratoire de Physique de la Matière Condensée
Ecole Polytechnique 91128 PALAISEAU Cedex

e-mail : bernard.sapoval@polytechnique.fr

Reprinted from "Fractals and Disordered Systems"
Armin Bunde - Shlomo Havlin (Eds.)
Springer-Verlag Berlin, Heidelberg, New York (1996) p. 233-261

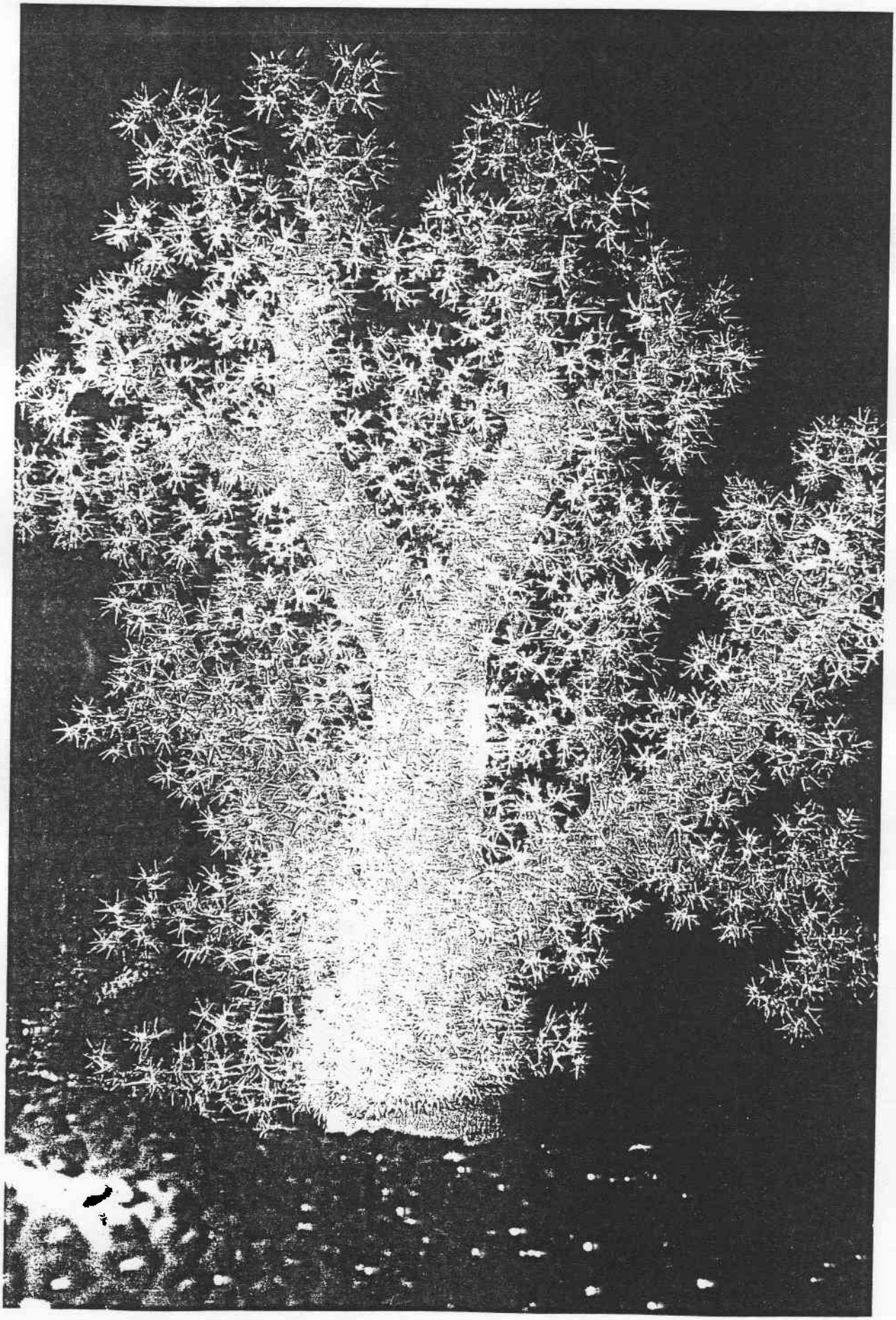

6 Transport Across Irregular Interfaces: Fractal Electrodes, Membranes and Catalysts

Bernard Sapoval

6.1 Introduction

How do irregular surfaces operate? This chapter is devoted to this general question, which has been revived by the concept of fractal geometry.

Many natural or industrial processes take place through surfaces or across the interfaces between two media. In this manner the roots of a tree exchange water and inorganic salts with the earth through their surface. Oxygen in the air is exchanged with blood hemoglobin through the surface of the pulmonary alveoli. These are natural processes.

In order for a car to start, the battery must deliver enough power to turn the engine, and a large current is needed for this purpose. In fact, the electrochemical process which supplies the current takes place at the interface between the electrode and the electrolyte. At this interface, the current is determined by elementary physical and chemical processes which limit its density. To obtain a large current it is necessary to increase the area of the exchange surface, and it is for this reason that *porous* electrodes are used. A porous medium is one which has a maximum surface area for a given volume. We know that fractal geometry qualitatively meets this criterion (the Von Koch curve has infinite length even though it is entirely contained within a finite surface [6.1–3]).

In this last example, the transport of the materials reacting in the electrolyte is due to electric current but it is possible to envisage similar processes involving no electric charge. Let us take the example of the lung: in the upper bronchial tube, air circulates hydrodynamically, but beyond this, in the alveoli, no air flows. The transport of oxygen to the cells which coat the pulmonary alveoli, where the gas exchange takes place, is a phenomenon of diffusion (see Sect. 3.2). Close to the membrane, the oxygen concentration in the air falls as the oxygen

◀ **Fig. 6.0.** Photograph of a soft coral, Solomon Islands, by Carl Roessler. Courtesy of C. Roessler

is trapped, and it is the diffusion of oxygen molecules in air which finally brings further molecules into contact with the membrane. Pulmonar alveoli have an irregular space-filling distribution [6.4–7] and fractal geometry can be used as a guideline.

We will show that these two problems, the current in a battery and breathing, can be solved using the same equations. The same applies to the absorption of a fertilizer through the roots of a plant, and other examples suggest that nature itself has perfected these systems by giving them a fractal geometry: "The problem of energy interchange in trees can be simplified by considering the tree as a system in which as large an area as possible must be irrigated with the minimum production of volume while at the same time guaranteeing the evacuation of absorbed energy" [6.8].

Again the same type of problem arises in heterogeneous catalysis. Solid catalysts are employed widely in the chemical and petroleum industries to promote many important chemical reactions. Porous catalysts are preferred since they can provide an enormous surface in a very small volume (up to several hundred square meters per gram) [6.9]. Reactants diffuse into the porous structure, reaction takes place, and the products formed diffuse back out to the ambient fluid.

The problem of transport to and across an irregular interface is thus a problem of general interest. It is of concern in studies in very different fields. We do not claim here that all irregular interfaces are indeed fractals. We first consider the question: if the interface is fractal what do we know about the transfer across such a surface? Once we have the answer to that question, we will see that it is possible to understand irregular interfaces in general. In the past fifteen years this field of research has been moving rapidly [6.10–60] but only recently can it be considered as settled and open to applications. It could appear in the future that the main applications of these results will exist in fields which are far from electrochemistry itself. Today, we can consider the following five conclusions as confirmed, and this is what I am going to describe and to discuss in this chapter.

1. The frequency response of a fractal electrode depends on the electrochemical regime.
2. In the so-called diffusion limited regime, the impedance of a fractal electrode depends directly on its Minkowski-Bouligand dimension. This will be shown in the following.
3. In the so-called blocking regime the response of a fractal electrode generally exhibits a nontrivial Constant Phase Angle (CPA) behavior. This behavior is directly related to the fractal hierarchy but the response of self-affine and self-similar electrodes are very different. In particular they do not depend on the fractal dimension in the same manner.
4. The macroscopic response of fractal interfaces is not proportional to the microscopic transport coefficients but is a power-law function of these pa-

rameters. This general property may be important because it may alter experimental measurements of the microscopic transport parameters.

5. We will show that there is an exact correspondence between the ac and dc electrical response of an electrode, the diffusive response of a membrane, and the steady-state yield of a heterogeneous catalyst of the same geometry. This is perhaps the most important result of this chapter. It unifies and widens the scope of applications of the study of transport to and across irregular interfaces. In particular we will see that the results can be applied to a semi-quantitative understanding of the absorption of oxygen into the blood in the terminal part of the respiratory apparatus of mammalians. In that sense the blocking electrode problem can be considered as a "model problem" offering the possibility of impedance spectroscopy measurements on model electrodes. It allows for a test of the various approximations which are necessary to understand simply the behavior of irregular interfaces. It is a means by which to validate ideas which may have their main future applications outside of the field of electrochemistry.

6.2 The Electrode Problem and the Constant Phase Angle Conjecture

The problem of transfer across a fractal surface was first addressed in the study of the impedance of batteries. It has been observed for a long time that rough or porous electrodes do not have a simple frequency response even in the small-voltage linear regime [6.61–66]. The equivalent circuit of a cell with planar electrodes of area S in principle consists of a surface capacitance C in parallel with the Faradaic resistance R_f, both being in series with the resistance of the electrolyte R_{el}. Figure 6.1 represents the electrical equivalent circuit of an electrochemical cell with planar electrodes.

The Faradaic resistance R_f is equal to (rS^{-1}) where r is the inverse rate of electrochemical transfer at the interface, for instance in a redox reaction such as

$$\mathrm{Fe}^{3+} + e^- \longleftrightarrow \mathrm{Fe}^{2+}. \tag{6.1}$$

In the absence of such a process the Faradaic resistance R_f is infinite and the electrode is said to be *blocking* or *ideally polarizable*. The resistance of the electrolyte R_{el} is proportional to the electrolyte resistivity ρ and depends upon the geometry of the cell. The surface capacitance $C = \gamma S$ is proportional to the surface area and to the specific capacitance per unit area γ. It corresponds to the charge accumulation across the interface. In the presence of such a Faradaic reaction it may happen that diffusion of the species in the liquid plays a role: such a case is termed a *diffusive regime* and appears at very low frequencies.

In fact, the impedance of rough or porous electrodes is generally found to be of the form

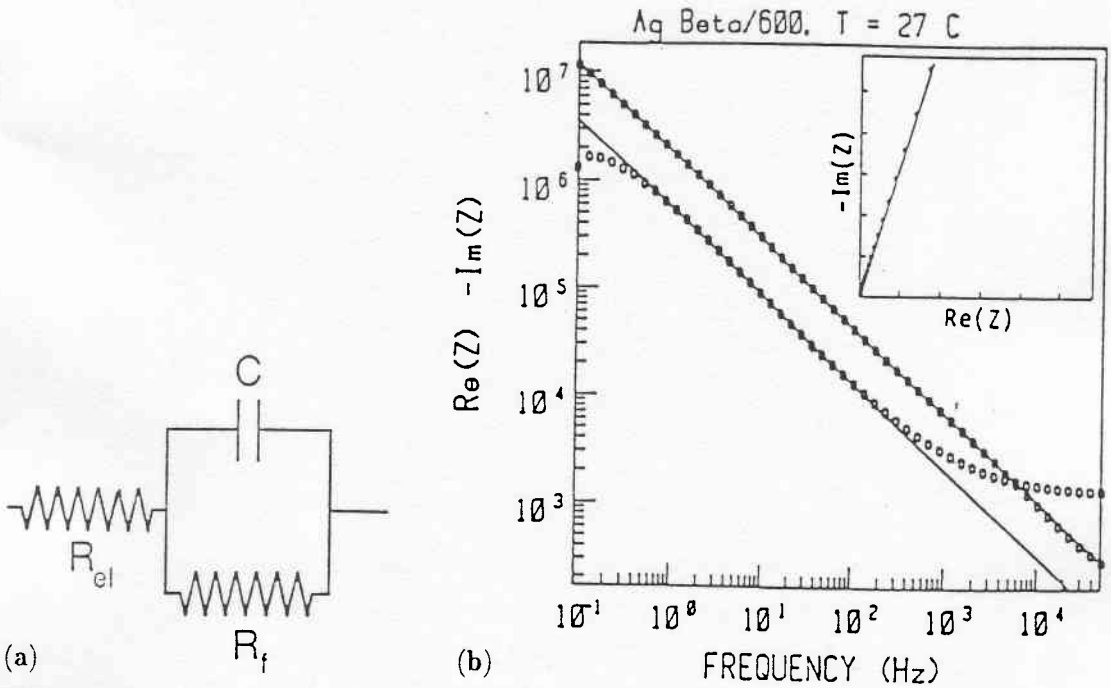

Fig. 6.1. (a) Equivalent circuit of a planar electrode in the small-voltage linear regime. (b) Experimental evidence for constant phase angle behavior obtained with metallic contacts on a solid electrolyte: sodium β-alumina [6.12]. Real and imaginary parts are measured as a function of frequency. The insert is an impedance diagram in the complex plane; it exhibits CPA behavior

$$Z \sim (i\omega)^{-\eta}, \quad 0 < \eta < 1, \tag{6.2}$$

in series with a pure resistance R_{el} which represents the resistance of the electrolyte. An example of such an experimental behavior is shown in Fig. 6.1b. This behavior is known as the constant phase angle or CPA behavior, because a plot of $-\mathrm{Im}Z(\omega)$ versus $\mathrm{Re}Z(\omega)$ in the complex plane gives a straight line with a "constant phase angle" with the x axis (as shown in the insert). There is a constant phase angle between the real and the imaginary parts. A smooth surface exhibits $\eta = 1$ (and a $\pi/2$ angle) whereas η decreases when the roughness of the surface increases.

Le Méhauté first proposed considering a rough or porous electrode as fractal, and many studies, the majority of them theoretical, have been devoted to this subject. These publications have mainly considered the properties of a blocking or ideally polarizable electrode. One should, however, keep in mind that there exist other interpretations of the CPA behavior which are not based on geometry. A suitable distribution of relaxation parameters on a flat surface can possibly account for CPA behavior [6.66 67]. Of course, both hierarchical geometry and these distributions can occur in real systems. We are interested here only in the role of the geometry because it is applicable to other phenomena: transport across membranes and heterogeneous catalysis.

At the beginning of these studies the emphasis was on searching only for a relation between the CPA exponent and the fractal dimension through scaling

arguments. We will see below that we now have analytical results from theory not only about exponents but also describing the response as a function of the geometrical and physical parameters which determine the system behavior. Although these results cannot be considered as "exact" from their derivation, which bears on a few approximations, they are in very good agreement with numerical simulations and explain quantitatively from first principles experiments on model electrodes.

6.3 The Diffusion Impedance and the Measurement of the Minkowski-Bouligand Exterior Dimension

We start with a consideration of a blocking electrode with a very small Faradaic transfer resistance. We recall that an electrochemical reaction (*Faradaic process*) may become diffusion limited whenever *indifferent* charged species (i.e., ions which are not participating in the electrochemical reaction) are present in the electrolyte simultaneously with the *electroactive* participating species. If a large concentration of indifferent charge species exists and a small potential step is applied, the interface capacitance will be charged after a very short time, because the solution is highly conductive, and the externally applied potential will then appear directly across the interface. A large initial Faradaic current will then flow, but this will change the concentrations of the electroactive species in the vicinity of the interface. Because the solution is highly conductive no electric field will be left and the only driving force bringing new electroactive species to the interface will be the concentration gradient, through a diffusion process. Consequently, a corresponding *diffusion impedance* appears in series with the (small) Faradaic resistance of Fig. 6.1a.

The concentration varies locally from c_0 to $c_0 + \delta c(x,t)$. The concentration profile $\delta c(x,t)$ will be governed by the diffusion equation in the sinusoidal regime ($\delta c(x,t) = \delta c(x) e^{i\omega t}$), which for a planar electrode is

$$i\omega(\delta c(x)) = D\frac{d^2(\delta c(x))}{dx^2}, \tag{6.3}$$

where D is the diffusion coefficient. The electrochemical current will be

$$J = -zeD\frac{d(\delta c(x))}{dx}\bigg|_{x=0} = ze(i\omega D)^{1/2}\delta c(x=0), \tag{6.4}$$

where $\delta c(x=0)$ is the variation of concentration at the surface, and z is the number of elementary charges per ion. Physically, this means that the charge passing through the interface during a cycle corresponds to the number of species at a concentration $\delta c(x=0)$ contained in a "diffusion layer" of thickness $\Lambda_D \sim (D/\omega)^{1/2}$. The associated admittance Y_D can be calculated by relating the concentration $\delta c(x=0)$ to the local potential by the Nernst law (see for

example [6.55] and references therein). For a planar electrode of area S one finds

$$Y_D = S\Gamma(D/i\omega)^{1/2} i\omega. \tag{6.5}$$

The quantity Γ is a capacitance per unit volume; we call it the specific diffusive capacitance [6.55]. This relation tells us that the diffusive admittance is simply that of the capacitance of the diffusive volume $S\Lambda_D \sim S(D/\omega)^{1/2}$. This can be readily extended to fractal surfaces.

The general form of the diffusion admittance at a fractal electrode can be found if we know the charge $\Gamma V(\Lambda_D)$ which is contained in the vicinity of the fractal electrode surface up to a distance of the order of $\Lambda_D \sim (D/\omega)^{1/2}$. We then need to know the volume $V(\Lambda_D)$ located within a distance Λ_D from the fractal surface. This is precisely what is measured by the *exterior Minkowski-Bouligand* dimension (here "exterior" means exterior to the electrode).

Let us now define this dimension. Let ϵ be a (small) positive length. Let V_ϵ denote the volume of electrolyte which lies within the distance ϵ of the electrode. Then

$$d_f = \lim_{\epsilon \to 0} \left(3 - \frac{\ln V_\epsilon}{\ln \epsilon} \right). \tag{6.6}$$

This definition is illustrated in Fig. 6.2.

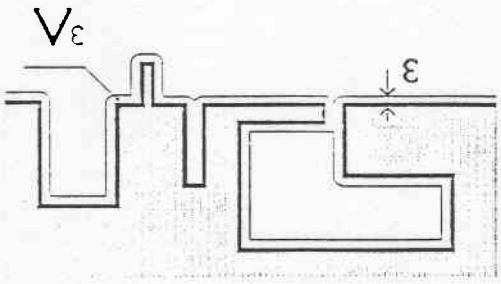

Fig. 6.2. Definition of the exterior Minkowski-Bouligand dimension. The contour of the electrode is the solid line. The electrode is shown in gray. The contour is "fattened" in the electrolyte by taking all points a distance smaller than ϵ away from the electrode (*thin line*). The volume V_ϵ is proportional to ϵ^{3-d_f} for an ordinary fractal surface

It is known that, for specific geometries, d_f may differ from the Hausdorff dimension of the common boundary of the electrode and electrolyte [6.68].

From (6.6) the volume $V(\Lambda_D)$ located within a distance Λ_D of the fractal varies as $\Lambda_D^{3-d_f}$, hence like $\omega^{(d_f-3)/2}$. The diffusion admittance of the fractal electrode is then $|Y_D| \sim \Gamma V(D/\omega)^{1/2}\omega \sim \omega^{(d_f-1)/2}$.

More precisely, if a fractal electrode has a macroscopic surface S, the content of the neighboring volume $V(\Lambda_D)$ is equal to $S^{d_f/2}\Lambda_D^{3-d_f}$, and one obtains

$$Y_D \sim S^{d_f/2} D^{(3-d_f)/2} c\, \omega^{(d_f-1)/2}. \tag{6.7}$$

Note that the response is given by a noninteger power law related to the fractal geometry. The above discussion fails at very low frequencies where the diffusion length may be larger than the size of the fractal electrode and reaches the size of the electrochemical cell. (For a solution of the problem in dc conditions see below.)

The very general reason allowing one to directly relate the ac diffusive regime to the fractal dimension is that, due to the presence of the support electrolyte, the volume of the electrolyte is electrically equipotential. The electrochemical potential is nonuniform on a scale of the order of the diffusion length. The reason for this nonuniformity is the electrical potential drop at the exchange surface. Since the electrical potential is uniform, this excitation is constant over the surface. As a consequence, the perturbation occurs only very close to the surface and the flux at some point on the surface is a local response. The ionic diffusion mechanism itself always takes place in the Euclidean space occupied by the electrolyte and is not perturbed by the presence of the fractal surface, which acts only as a boundary. It is therefore not surprising that this flux can be related to some dimension through a *fattening* of the surface as done in the Minkowski-Bouligand approach. More generally, the content of a Minkowski-Bouligand layer of thickness Λ_D permits one to describe the impedance of any irregular, rough or porous, fractal or nonfractal interface in the diffusive regime. These effects have been thoroughly studied together with the time response (Cotrell law) of these electrodes and verified by numerical simulations and experiments [6.46,47,49–51,55].

On the other hand, if the resistance of the electrolyte plays a role, as in the case discussed previously of blocking electrodes, the electrolyte is no longer equipotential and the response is no longer local. In that case, the admittance is not related to the local properties of the interface as characterized by the fractal dimension. This will be shown first in a specific case where the response of a model electrode can be calculated exactly: the *generalized modified Sierpinski electrode*. Our calculation would also be applicable to a catalyst of the same geometry as will be shown later.

6.4 The Generalized Modified Sierpinski Electrode

This electrode is the metallic electrode shown in Fig. 6.3. It is made in a decimation process. In the first step, a square pore of side a_0 is made in the electrode of side a. Then, at each step, N smaller pores of side a_0/α are added around a pore of a given size and so on. Here $N = 4$ and $\alpha = 3$. A cross section of the electrode is a modified Sierpinski carpet with a fractal dimension in the plane $d_{f,p} = \ln N / \ln \alpha$. We consider the case where:

1. The other electrode of the electrochemical cell is planar. It is very near the fractal electrode so that one can neglect the resistance of the thin layer of electrolyte between the two electrodes.

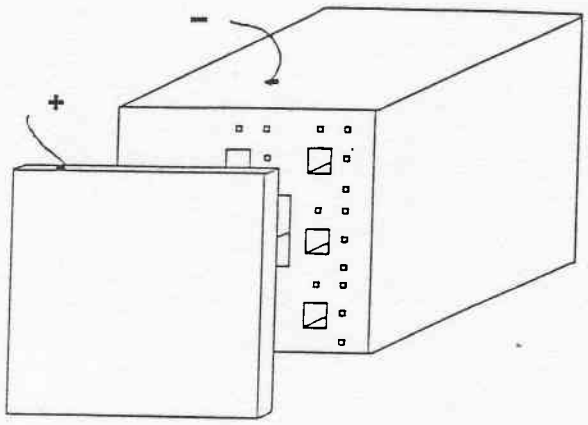

Fig. 6.3. Picture of the generalized modified Sierpinski electrode in front of a planar counter electrode. The fractal object that we consider is made by a decimation process. In the first step a square pore of side a_0 and depth L is made in the electrode of side a. Then, at each step, N smaller pores of side a_0/α and depth L/α_z are added around a pore of a given size, and so on. Here $N = 4$ and $\alpha = 3$. For this model electrode, exact results can be obtained for various electrochemical regimes [6.55]

2. The metallic volumes are assumed to have zero resistance and the external surface is coated with an insulating material so that we neglect conduction through this surface.
3. The bottom of each pore is insulating. All the pores are linked in parallel and the admittance is simply the sum of the admittances of all the pores.
4. The lengths of the pores also scale (either as the side of the pores or differently). Hence, the largest pore has a length L, the next pores have a length L/α_z and so on. For example, thinner pores can be shorter than thicker pores.

This electrode really has a self-affine geometry (see Chap. 7). It has an infinite surface area included in a finite volume. Its exterior Minkowski-Bouligand dimension can be easily calculated as we now show. We have N^n pores of length $L\alpha_z^{-n}$ and of side $a_0\alpha^{-n}$. The fact that the electrode occupies a finite volume implies $N \leq \alpha^2$. To calculate the dimension, we choose a small positive length ϵ and separate the pores with sides smaller and greater than ϵ. For this we find the order of decimation ν of the pore side ϵ. The quantities ϵ and ν are related by

$$\alpha^{-\nu-1}a_0 < \epsilon/2 < \alpha^{-\nu}a_0. \tag{6.8}$$

We then have

$$V_\epsilon \sim \sum_{n=\nu}^{\infty} N^n a_0^2 L(\alpha^2\alpha_z)^{-n} + 4\epsilon \sum_{n=0}^{\nu-1} N^n a_0 L(\alpha\alpha_z)^{-n}. \tag{6.9}$$

There are two possibilities. First $N > \alpha\alpha_z$. Then the second term is of the order of magnitude of $\epsilon N^\nu a_0 L(\alpha\alpha_z)^{-\nu}$, and the first term is equivalent to $N^\nu a_0^2 L(\alpha^2\alpha_z)^{-\nu}$. Remembering (6.8), ν is of order of $\ln(a_0/\epsilon)/\ln\alpha$ and we get $V_\epsilon \sim \epsilon^{2-\ln N/\alpha_z)/\ln\alpha}$, and from (6.6)

$$d_f = 1 + \frac{\ln N - \ln \alpha_z}{\ln \alpha}. \tag{6.10}$$

Note that if $\alpha_z = 1$, all the pores have the same depth and $d_f = 1 + \ln N / \ln \alpha$. In the case where $N \leq \alpha\alpha_z$, the dimension is 2. As a result of the simple geometry, several electrochemical regimes have been calculated for the generalized modified Sierpinski electrode [6.55].

We show now that the generalized modified Sierpinski electrode exhibits CPA response in the blocking regime, but the CPA exponent is not a function of the fractal dimension. The pores are branched in parallel and the total admittance is simply the sum of the admittance of the individual pores,

$$Y = \sum_{n \geq 0} N^n Y_n. \tag{6.11}$$

In a first approximation, a single pore can be considered as a resistance R_n in series with a capacitance C_n, if one neglects propagation effects. The quantities R_n and C_n are the resistance and the surface capacitance of a pore of order n. These pores have a length $L/(\alpha_z)^n$ and a side a_0/α^n. Hence:

$$R_n = \rho(L/\alpha_z^n)(a_0^{-2}\alpha^{2n}) \tag{6.12}$$

and

$$C_n = 4\gamma(a_0/\alpha^n)(L/\alpha_z^n). \tag{6.13}$$

There are N^n such circuits in parallel for each stage of decimation. It can be easily verified that at a given frequency ω the admittance is dominated by the pores with $R_n C_n \omega = 1$, that is, those for which the order of decimation is $n(\omega)$ such that [6.55]

$$4\rho\gamma(L^2/a_0)(\alpha/\alpha_z^2)^{n(\omega)} = \omega^{-1} \tag{6.14}$$

or

$$n(\omega) = \frac{\ln(a_0/4\rho\gamma\omega L^2)}{\ln(\alpha/\alpha_z^2)}. \tag{6.15}$$

For these pores the resistive and capacitive admittances are equal and the admittance is then of the order of

$$|Y| \sim N^{n(\omega)} R_{n(\omega)} \sim (a_0^2/\rho L)(a_0/4\gamma\rho L^2)^{-\eta}\omega^{\eta}, \tag{6.16}$$

with

$$\eta = \frac{\ln N + \ln \alpha_z - 2\ln \alpha}{2\ln \alpha_z - \ln \alpha}. \tag{6.17}$$

Hence there exists a CPA response but the exponent η is not a function of the fractal dimension (6.10) of the interface. This constitutes an *exact* result. In that very special geometry there is no direct relation between the dimension and the phase angle. Note that the function (6.16) is a nontrivial function of a_0, ρ, γ, L, and ω. The admittance is dominated by the $n(\omega)$ pores of characteristic frequency ω and the energy is dissipated in these particular pores. On such fractal interfaces the power dissipation is nonuniform.

Keddam and Takenouti [6.31] have studied the frequency response of a two-dimensional Koch electrode made of anodized aluminum. That is a case where

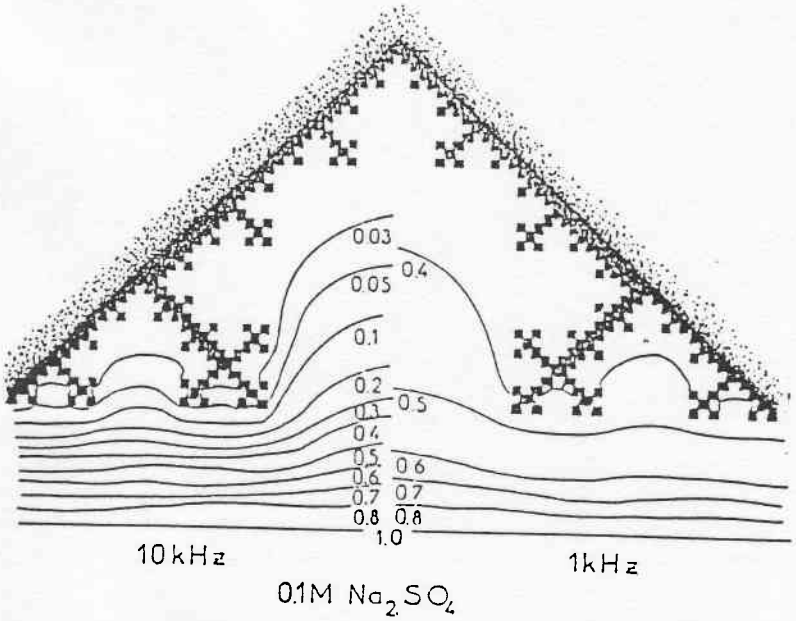

Fig. 6.4. Experimental map of the ac electric potential for two different frequencies in a fractal electrochemical cell, after Keddam and Takenouti [6.31,74]. The potential is 1 on the bottom horizontal line. Equipotential lines are shown for 10kHz in the left part and for 1Hz in the right part. The electrode is made of an oxidized aluminum profile and is blocking in the Na_2SO_4 solution where the measurement is made. One observes a stronger penetration of the ac potential in the structure at lower frequencies. This is related to the higher value of the surface capacitive impedance at low frequencies. These maps indicate qualitatively that the different parts of a fractal object do not play the same role in the blocking regime [6.60,83,84,86]. This must be contrasted with the diffusive regime response that we have studied above and where the active zone is evenly distributed on the surface as shown in Fig. 6.2

the electrode is really a "blocking" electrode. They have studied the potential distribution in that case and have demonstrated that the equipotential lines in the electrolyte penetrate the fractal object in a nonuniform manner which depends on the frequency. This is shown in Fig. 6.4.

The idea of a nonuniform role of the fractal surface was independently discussed by Wang [6.60] and will be discussed below.

6.5 A General Formulation of Laplacian Transfer Across Irregular Surfaces

We describe now a simple way to consider and to compute the impedance of irregular interfaces using a simple and general argument [6.69]. It applies to any irregular electrode and in particular to self-similar electrodes. In addition it permits us to compute the response from the geometry of the interface only.

In the electrochemical cell the potential obeys the Laplace equation [6.70,71]. The method is to substitute the problem of Laplacian transfer across the real

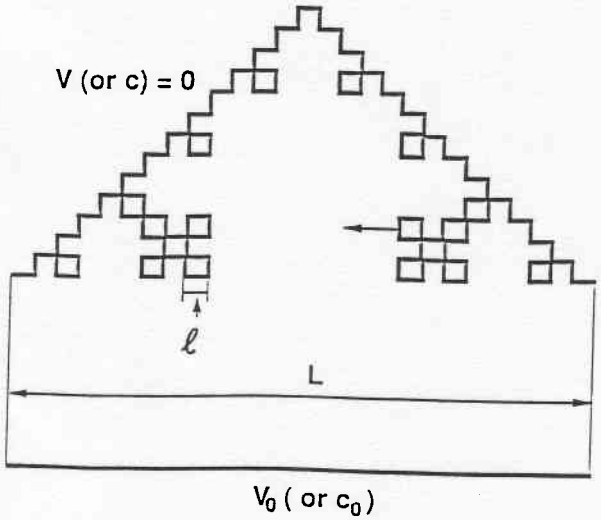

Fig. 6.5. Electrochemical cell with a self-similar electrode. The irregular electrode of interest (the working electrode in electrochemistry) has an inner cut-off ℓ and size or diameter L. The arrow indicates the orientation of the normal. This chapter deals with the electrochemical problem in which the applied voltage is V_0 on the planar counter electrode and 0 on the working electrode. An equivalent diffusion problem exists in which a planar source of diffusion is maintained at a constant concentration c_0 and particles diffuse towards an irregular membrane with finite permeability W

electrode (which presents a finite transfer rate) by a problem of a Laplacian field obeying the Dirichlet boundary condition ($V = 0$) but with a different geometry, obtained by coarse graining. The coarse-graining scale is directly related to the transport coefficients of both the electrolyte and the electrode. Using general properties of Dirichlet-Laplace fields one finds an effective screening factor which gives the size of the zone being really active on the initial geometry, and hence its admittance.

To calculate the response of an electrochemical cell with an irregular electrode, as in Fig. 6.5, one has to solve the Laplace equation ($\Delta V = 0$) which governs the electric potential distribution in the electrolyte with a boundary condition that reflects the electrochemical process at the working surface. This surface possesses a finite admittance and what is known about the properties of Laplacian fields on surfaces without impedance (with $V = 0$) cannot be applied directly. This is unfortunate since the Dirichlet-Laplace problem on an irregular electrode has been thoroughly studied, at least in $d = 2$. More specifically an important theorem, Makarov's theorem, describing the properties of the charge distribution on an irregular (possibly fractal) electrode capacitor can be applied [6.72]. This theorem states that the information dimension of the harmonic measure (for instance the electrostatic charge for the capacitor case) on a singly connected object in $d = 2$ is exactly equal to 1. This very special property of the Laplacian field can be illustrated in the following manner: whatever the shape of an capacitor electrode, the size of the region where the charge accumulates is proportional to the overall size (or diameter) L of the electrode under a dilation transformation.

This result generalizes, to an arbitrary geometry, a fact which has been known for a long time for simple geometries. It has a profound meaning in terms of the screening efficiency of the irregularity and this is what we use. For this, we consider the simplest description of an irregular surface: the length of the perimeter L_p divided by its size or diameter L [6.73].

$$S = L_p/L. \tag{6.18}$$

This number S has a direct significance: it measures the screening efficiency of the irregularity for Dirichlet-Laplacian fields: If whatever the geometry the active zone has a size L, then as

$$L = L_p/S \tag{6.19}$$

the factor $1/S$ can be considered to be the "screening efficiency" due to the geometrical irregularity. This is the physical significance of Makarov's theorem. (Note that when we discuss fractal lines we consider only physical objects with a finite inner cut-off ℓ so that S is always finite.)

The above result cannot be applied directly to the screening of the current in an electrochemical cell because the boundary condition on the electrode is not $V = 0$. In the simplest linear regime, a "flat" element of an electrode surface with unit area behaves as a resistor r across a capacitance γ. The Faradaic resistor r describes the finite rate of the electrochemical reaction if the interface is not blocking. Due to charge conservation, the current $j_\perp = -V(r^{-1} + j\gamma\omega)$ crossing the electrode surface must be equal to the Ohmic current $j_\perp = -\nabla_\perp V/\rho$ reaching it from the bulk (ρ being the electrolyte resistivity). As a consequence the dc boundary condition can be written as

$$V/\nabla_\perp V = \Lambda \quad \text{with} \quad \Lambda = r/\rho. \ * \tag{6.20}$$

This boundary condition then introduces a physical length scale Λ in the problem. The procedure that we describe now is to switch from the real geometry obeying the real boundary condition to a coarse-grained geometry obeying the Dirichlet boundary condition, with the coarse-graining depending on Λ. In that new geometry we will apply equation (6.19) to obtain the effective screening, hence the size of the working zone of the real electrode.

To be more specific we describe this analysis for the situation of an electrode in a planar $d = 2$ cell as represented in Fig. 6.5. Consider a part i of the surface with a perimeter length $L_{p,i}$. If the thickness of the cell is b, this surface possesses an admittance $Y_i = bL_{p,i}/r$. The admittance to access the surface is of order $Y_{acc} = b/\rho$ because in $d = 2$ the admittance of a square of electrolyte with thickness b is equal to b/ρ whatever its size. Depending on the size of the region i there exists two situations: $Y_i < Y_{acc}$ or $Y_i > Y_{acc}$. If $L_{p,i}$ is small, $Y_i < Y_{acc}$ and the current is limited by the surface admittance. On the contrary if $L_{p,i}$ is large enough we have $Y_i > Y_{acc}$ and the current is limited by the resistance to access the surface. But in the latter situation we are, in a first approximation,

* The length Λ is equivalent to the lenght k_c defined by Carl Wagner, J. Electrochem. Soc., 98, 116 (1951). See also T. P. Hoar and J. N. Agar, Disc. Faraday Soc., 1, 162 (1947) and C. Kasper, Trans. Electrochem. Soc., 77, 353 (1940); 78, 131 (1940; 812, 153 (1942)

back to the case of a pure Laplacian field with the boundary condition $V = 0$. The idea then is to coarse-grain the real geometry to a scale $L_i = L_{cg}$ such that the perimeter $L_{p,cg}$ in a region of size (diameter) L_{cg} is given by the critical condition $Y_i = Y_{\text{acc}}$ or

$$L_{p,cg} = \Lambda. \tag{6.21}$$

A coarse-grained site is then a region with a perimeter equal to $\Lambda = r/\rho$. Because of its definition, such a region can be considered as acting uniformity. At the same time, in the new coarse-grained geometry we are dealing with a pure Dirichlet Laplacian field and we can then use the screening factor $1/S_{cg}$ of this object to find its effective active surface. Note that if we did the coarse-graining to a scale larger than L_{cg} it would no longer be correct to consider a uniform distribution of the current within a macrosite and that consequently we would not be able to find the size of the active zone. If N_p is the number of yardsticks of length L_{cg} needed to measure the perimeter of the electrode, the number S of the coarse-grained object is simply

$$S_{cg} = N_p/N, \tag{6.22}$$

where $N = L/L_{cg}$ is the number of yardsticks needed to measure the size (or diameter) of the electrode. The quantity $1/S_{cg}$ is the effective fraction of the surface which is active and the admittance of the electrode will simply be given by

$$Y(r) = Y_p(r)/S_{cg}, \tag{6.23}$$

where $Y_p(r)$ would be the surface admittance of a "stretched" electrode with a length L_p. In this frame the number S_{cg} of the coarse-grained object determines directly how the admittance of the total surface is reduced by the screening effects. If we consider a self-similar electrode with an inner cut-off ℓ and a fractal dimension d_f there exists a simple relation between the size L_{cg} of the coarse-graining and the length of the perimeter:

$$\Lambda = \ell(L_{cg}/\ell)^{d_f}. \tag{6.24}$$

Using (6.21–24) one obtains for the admittance of a self-similar electrode of macroscopic size L and thickness b the value

$$Y = Lb(\ell\rho)^{(1-d_f)/d_f} r^{-1/d_f}. \tag{6.25}$$

The general (nonblocking) ac response is obtained by substituting r by $(r^{-1} + j\gamma\omega)^{-1}$

$$Y(\omega) = Lb(\ell\rho)^{(1-d_f)/d_f}(r^{-1} + j\gamma\omega)^{1/d_f}. \tag{6.25a}$$

For blocking electrodes with $r^{-1} = 0$ we have

$$Y(\omega) = Lb(\ell\rho)^{(1-d_f)/d_f}(j\gamma\omega)^{1/d_f}. \tag{6.26}$$

The dc form of this result has been verified by numerical simulation and the ac form has been verified by experiments on model electrodes as described in detail in reference [6.74].

At very low frequency, where the size of the coarse-grained site is larger than the diameter of the system, the admittance is limited by the capacitance of the total surface and

$$Y(\omega) = Y_p(\omega) = \ell b (L/\ell)^{d_f} (j\gamma\omega). \tag{6.27}$$

The high-frequency fractal regime and the low-frequency capacitive regime meet at a cross-over frequency ω_c where the size of the coarse-graining is the size or diameter L of the electrode itself. For a blocking electrode $\Lambda = (\rho\gamma\omega)^{-1}$ and (6.24) gives for this crossover

$$\omega_c = (\rho\gamma\ell)^{-1}(L/\ell)^{-d_f}. \tag{6.28}$$

The above simple arguments are general and permit, as we show below, the computation of the response of irregular electrodes even for nonscaling geometries. First we show how this method can be used from the image of the electrode. All we need is to have a "flexible" measuring rod of length $\Lambda = r/\rho$ (or $|\Lambda(\omega)| = 1/\rho\gamma\omega$ for blocking electrodes) that we use to measure the length of the perimeter from one end to the other. To perform this task we need a number N_p of flexible rods. Note that here, we do not measure the irregular object with a rigid yardstick as usually considered in measuring fractals. On the contrary, starting at one end of the irregular object, we map the object with the flexible rod of length Λ and the distance in real space between the ends of this rod determines a distance L_1. This length is a "local yardstick" associated with Λ and the local geometry. Then we place a second flexible rod of length Λ from the end of the first rod and find a new yardstick length L_2 and so on. The total number of rods (of length Λ) needed to map the object is N_p and the number S of the coarse-grained electrode is N_p/N where N is the number of yardsticks which measure the size. The real electrode has a perimeter $N_p\Lambda$ and a total admittance $Y_p(r) = N_p\Lambda b/r = N_p b/\rho$. Dividing by S as in (6.23) we find

$$Y = Nb/\rho. \tag{6.29}$$

We then obtain that the modulus of the admittance of an irregular electrode in $d = 2$ is simply the square admittance b/ρ multiplied by the number of yardsticks needed to measure the size (or diameter) L of the electrode. This shows that deterministic and random fractals with the same inner and outer cut-offs and the same fractal dimension have the same response. The reason is now trivial because what really matters is the total number of macrosites, whatever their individual size, which may be distributed over some range of sizes.

We now apply this method to nonscaling geometries as shown in Fig. 6.6. The dc admittance of the perimeter surface is now $Y_p = (N'_p + N''_p)b\Lambda/r$ with

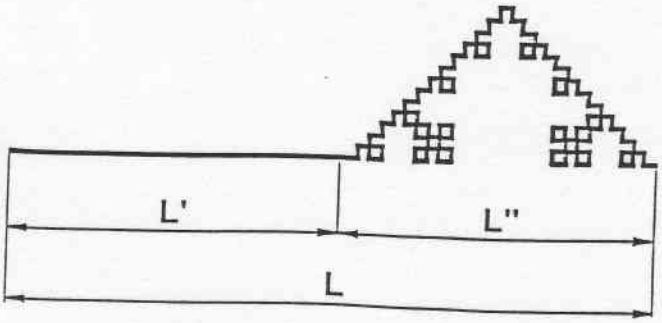

Fig. 6.6. Example of an electrode with a nonscaling geometry. This electrode is build by the association of a planar electrode of length L' with a self-similar electrode of length L''

$N'_p = L'/L'_{cg}$ and $N''_p = (L''/L''_{cg})^{d_f}$. To obtain the admittance of this electrode we have to divide this value by S of the entire electrode. The macrosites do not have the same size if they correspond to the planar part, for which the yardstick is simply $L'_{cg} = \Lambda$, or if they corresponds to the fractal part for which the yardstick is given by $L''_{cg} = \ell(\Lambda/\ell)^{1/d_f}$ from (6.24). The total number of yardsticks on the object is now $N_p = N'_p + N''_p$, whereas the number of yardsticks needed to measure the size is $N = N' + N''$ with $N' = L'/L'_{cg}$ and $N'' = L''/L''_{cg}$. Applying (6.23) with $S = (N'_p + N''_p)/(N' + N'')$ one finds for the admittance $Y = (N' + N'')b/\rho$ or $Y = L'b/r + L''b(\ell\rho)^{(1-d_f)/d_f} r^{-1/d_f}$, which is the sum of the admittances of the two electrodes in parallel.

This general argument then restores the essential property of Laplacian transfer: the admittance of two electrodes in parallel is the sum of the individual admittances. This indicates that this method is general. The ac response of blocking electrodes is obtained by replacing r by $(j\gamma\omega)^{-1}$. Note that we have used the number N of yardsticks needed to measure the total size as equal to the sum $N' + N''$ of the number of yardsticks needed to measure the sizes of the two different parts. If we wish to use equation (6.29) we have to use an average yardstick $\langle L_{cg} \rangle$ defined by $L/\langle L_{cg} \rangle = L'/L'_{cg} + L''/L''_{cg}$. The average yardstick $\langle L_{cg} \rangle$ must be obtained by this harmonic mean.

In the known cases of self-affine electrodes, such as the Cantor bar electrode [6.38–40] or the Sierpinski electrode studied above, the pores have different aspect ratios. For this case a coarse-grained pore can be still defined by $Y_i = Y_{acc}$ but not by $L_{p,cg} = \Lambda$. As explained above in a somewhat different language the impedance can be found from the total surface of these coarse-grained pores, which are all accessible at the same time due to the particular geometry.

We then have shown how to find, from first principles, the response of a nonscaling irregular object. Apart from the image, all that is needed are the values of the microscopic transport coefficients (here, for instance, the electrolyte resistivity and the Faradaic resistance). The same method will apply to the equivalent problem of the steady-state diffusion rate towards an irregular membrane with finite permeability Π as indicated below.

The simplicity of this method probably makes it a good candidate for the study of the response of irregular electrodes in the nonlinear regime where the local current across the electrode is related to the local voltage by a non nonlinear relation $j = f(V)$ [6.47,69,75].

The case of self-similar electrodes with $2 < d_f < 3$ (in $d = 3$) has been treated by an equivalent circuit method in [6.74] and gives, respectively, for the high-frequency fractal and low-frequency capacitive regime

$$Y(\omega) = L^2(\ell\rho)^{(d_f-2)/(1-d_f)}(j\gamma\omega)^{1/(d_f-1)}, \tag{6.30}$$

and

$$Y(\omega) = \ell^2(L/\ell)^{d_f}(j\gamma\omega). \tag{6.31}$$

The crossover frequency ω_c is now

$$\omega_c = (\rho\gamma\ell)^{-1}(L/\ell)^{1-d_f}. \tag{6.32}$$

Note that in this case the crossover frequency occurs when the perimeter of a cut of the fractal surface by a plane is equal to the length Λ. These theoretical predictions allow us to explain quantitatively the high-frequency and low-frequency response of the electrode shown in Fig. 6.7 [6.76,77].

We have presented here a simple approach based on first principles. These results have been verified by the existing numerical simulations in $d = 2$ and permit us to understand quantitatively the experimental results in $d = 2$ and $d = 3$. A different and more complex approach has been proposed in [6.78–82]. These more detailed studies present slightly different values for the exponent $\eta = \tau(2)/d_f$ using a correlation exponent $\tau(2)$ slightly < than 1. In this situation, one should consider that the above results (6.25-28) and (6.30-32) allow us to grasp the essential features of that question.

Another significant result from the equivalent circuit approach of [6.74] and from [6.83.84.86] is the notion of information fractal and of active zones. The active-zone studies give a direct insight on the localization of the regions which are effectively working and those which are passive for given physical conditions. This is a further step in the detailed understanding of how irregular interfaces operate in the linear regime. This notion could be of great help in the understanding of how irregular interfaces operate in a nonlinear regime [6.69].

The above discussion about screening indicates that if one considers self-affine electrodes in the case where the aspect ratio of the groves is smaller than 1 there is no effect and no CPA. The experiments of Bates, Chu, and Stribling [6.13] are, from this point of view, experiments on self-affine electrodes with small aspect ratios. From the discussion about S numbers in that case, the response should be capacitive. This is why they do not obtain any relation between fractal dimensions and the CPA exponents. In their case the CPA may be due to microscopic effects.

In this chapter we have assumed that no dc polarization current is flowing in the system, which is far from being the case in very many practical elec-

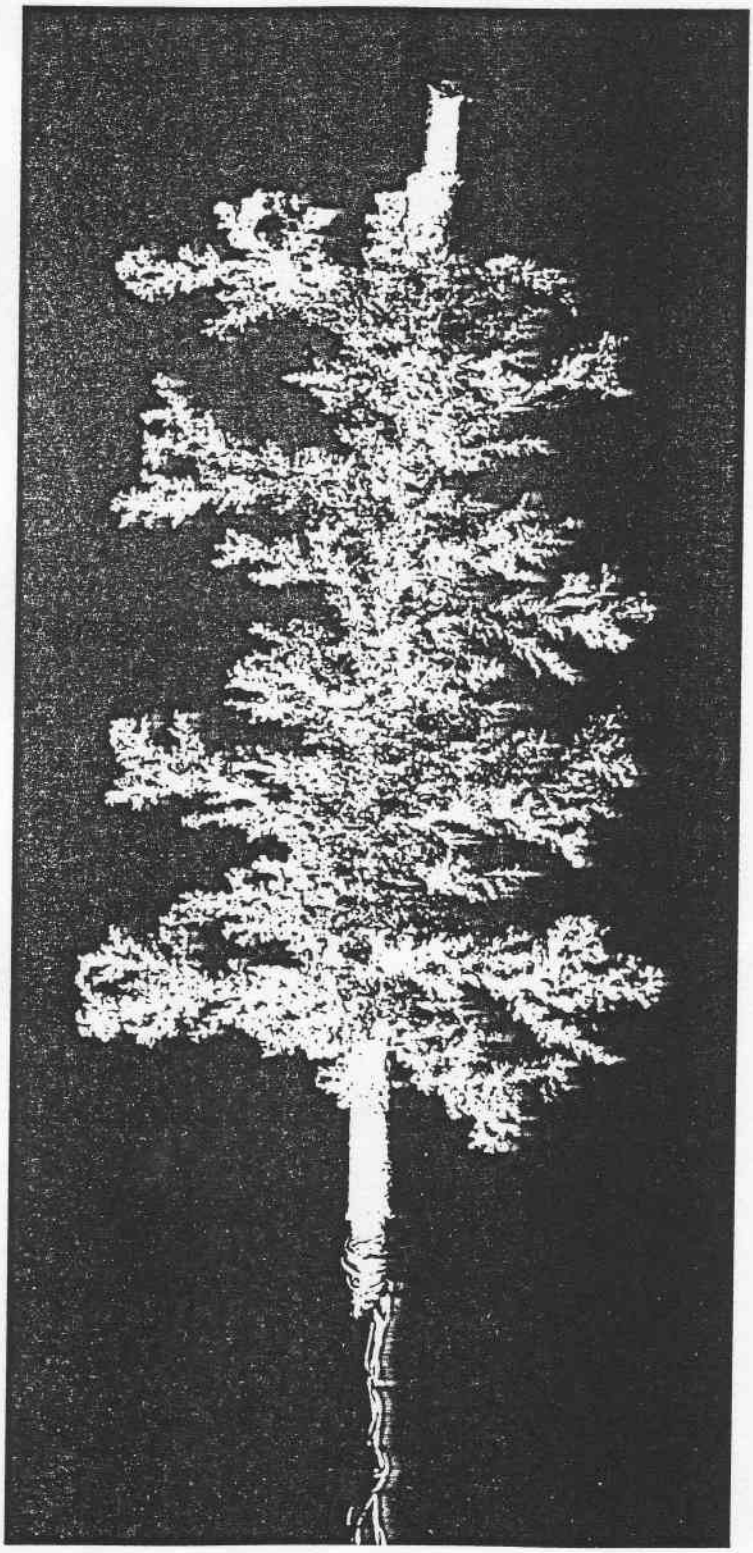

Fig. 6.7. Wood's metal ramified electrode. This object is approximately 6 cm high and has its smallest branching in the range of 20μm. It is a metallic moulding of the penetration space of water injected into plaster and was obtained by G. Daccord and R. Lenormand [6.77]. In a blocking situation the admittance of this electrode approximately obeys relations (6.30-32)

trochemical situations. The presence of a dc polarization current would make the (potential-dependent) Faradaic admittance vary from one point of the interface to another. This would complicate the problem considerably, and most probably the results would be affected.

6.6 Electrodes, Roots, Lungs, ...

The dc admittance given by (6.25) is proportional to $r^{-\eta}$. This result is not trivial. It means, for instance, that dividing the surface resistance at the surface of a porous electrode by a factor of two will not double the current. Also the current is not proportional to the electrolyte conductivity but is a power law of the conductivity. As a result, the macroscopic response coefficient across a fractal interface is not proportional to the microscopic transport coefficients. A power law depending on the geometrical hierarchy relates these factors. This conclusion could have applications in several systems found in nature or those built to have large-surface porous structures.

The same kinds of properties should be observed in the study of bulk and membrane diffusion that exists in biological or physiological fractal systems. We now illustrate the correspondence between the above study and the description of the flux of a neutral species across a membrane when the overall process is limited by the diffusion from a source at a constant concentration. Consider the mathematical problem of finding the dc response in the electrochemical cell of Fig. 6.8a.

The potentials are V_0 on the counter electrode and $V = 0$ on the electrode of interest. As we have seen, the equations to be solved are the Laplace equation and the current equation in the bulk of the electrolyte with the boundary

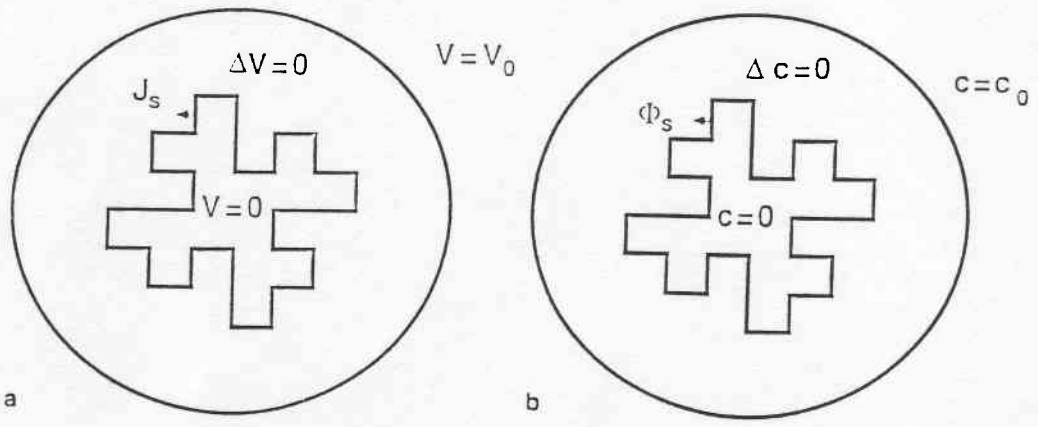

Fig. 6.8a,b. Equivalence between the electrode problem and the membrane problem in the same geometry. If one replaces Φ by J, c by V, D by ρ^{-1}, and W by r^{-1} one obtains the same mathematical problem for a given geometry

condition for the electrical current normal to the surface. Instead of an electrochemical problem we imagine the problem of the transfer of neutral species diffusing across a membrane of the same geometry. Instead of a counterelectrode as in Fig. 6.8a we imagine that some process maintains a constant concentration c_0 of the species of interest. This is the situation of Fig. 6.8b. We call Φ the flux vector at point x. There are two flow processes in our system. First, diffusion, which in a steady state obeys Fick's law,

$$\Phi = -D\nabla c(x), \tag{6.33}$$

where c is the concentration of the particles of interest and D is the diffusion coefficient, as before. Together with the conservation law

$$\frac{\partial c}{\partial t} = -\nabla\Phi \tag{6.34}$$

this leads to the diffusion equation, which in a steady state is

$$\Delta c = 0. \tag{6.35}$$

Second, there is a transfer equation across the membrane,

$$\Phi_n = -Wc(x), \tag{6.36}$$

where W is the probability per unit time, surface, and concentration of a particle crossing the membrane. In the last equation we have neglected a back transfer, assuming that the concentration on the other side of the membrane is maintained equal to zero by some forced flow mechanism (blood circulation for example in the case of lungs). Provided that we replace Φ by J, c by V, D by ρ^{-1}, and W by r^{-1}, relations (6.33,35–36) are exactly equivalent to the dc current and potential equation in the electrochemical cell. The same results do then apply. If we define a diffusion admittance Y_D by a linear relation between the total flux Φ_T and the concentration c_0 at the entrance of the system we can write

$$\Phi_T = Y_D c_0 \tag{6.37}$$

Note that one should not confuse the steady-state diffusion regime that we study here and the so-called diffusion electrochemical regime that we have discussed in Sect. 6.3. This last regime was the time-dependent response of the electrode in the special case where the electric field is screened by the presence of a large concentration of inert (indifferent) electrolyte. The equivalence that we use here is between a steady-state diffusion regime and the Laplacian response of an electrode with the same geometry.

By transposition of (6.30–32) to the steady-state diffusion case one obtains a low-permeability regime with a diffusion admittance, which trivially is

$$Y_D = \ell^2 (L/\ell)^{d_f} W, \tag{6.38}$$

and a high-mobility "fractal" regime with a diffusion admittance equal to

$$Y_D = L^2 \ell^{(d_f-2)/(1-d_f)} D^{(d_f-2)/(d_f-1)} W^{1/(d_f-1)}. \tag{6.39}$$

Here also the macroscopic response is a power law of the transport coefficients D and W. The value of the length Λ is now $\Lambda = D/W$ and the crossover between the two regimes occurs when

$$\Lambda = \ell (L/\ell)^{(d_f-1)}, \tag{6.40}$$

which is when the perimeter of a cut of the fractal surface by a plane is equal to the length Λ.

Note that at crossover, the value of the membrane admittance needed is equal to the value of the admittance to reach the surface, which, in $d = 3$ is typically the (bulk) admittance of a cube of size L: $Y_B = LD$. The statement that, at the crossover point, the value of the classical admittance of the fractal membrane is equal to the access resistance is very simple. It may then be of more general value and may apply to many irregular geometries. That is probably why the above considerations seem to apply to the "acinus" of several animals, as discussed now, although their real geometry is not a simple fractal [6.6.7].

The airways of mammalians are made of two successive systems, the bronchial tree in which oxygen is transported with air and the terminal alveolar system, called the acinus, in which the air does not move. In the acinus the transport of oxygen towards the alveolar membrane is purely diffusive. In this system the transport may be limited both by the (bulk) diffusion admittance to reach the membrane and the admittance needed for the air of the membrane itself as given by (6.38,39). In $d = 3$ the bulk admittance is equal to LD and the total admittance is

$$Y_T = ([LD]^{-1} + Y_D^{-1})^{-1}. \tag{6.41}$$

This admittance increases with the diameter L and large exchangers should trivially be better exchangers. But the "best" exchange system should be that for which it is not the admittance itself but the admittance per unit volume, as the thorax volume of animals is limited. The above discussion indicates that the admittance per unit volume or specific admittance, defined as $Y_T/L^3 = ([LD]^{-1} + Y_D^{-1})^{-1}/L^3$, varies as L^{d_f-3} for small L and as L^{-2} for large L. If the structure of the alveolar surface is dense, $d_f = 3$ and the specific admittance does not depend on the size of the fractal up to the critical size discussed above but decreases with the power L^{-2}. From this discussion a geometry with a dense (space filling with $d_f = 3$) arrangement of alveolar surface of smaller size ℓ, up to a diameter L satisfying condition (6.40) should be optimum because lower losses in the higher airways ask for the larger size compatible with a large

specific admittance. In that sense the "best possible acinus" size should be that for which the perimeter of a cross section through the acinus should have a length of the order of Λ. The physiological and anatomical data obtained by E. Weibel [6.5–7] allows us to compare the above considerations with what is observed in real lungs. The transport coefficients D and W governing the diffusion of oxygen in air and its capture by the alveolar membrane are known and it seems that the value of Λ (a few cm) is indeed close to the perimeter length of a cross section through the acinus for several animals such as the mouse, the rat, the rabbit, and the human. Although discrepancies exist, the general agreement can be considered as satisfactory if one takes into account the oversimplified model that is used [6.85].

It seems that these considerations can be extended to the gills of fish, in which the geometry is regular. Because of the smaller diffusion coefficient of oxygen in water, the value of Λ is of the order of a few tens of micrometers. The size of the gills is comparable to that value. The gills generally have a regular structure which corresponds to $d_f = 2$ and not to $d_f = 3$ [6.87]. In that case the optimum value for L is equal to Λ, now of the order of tens of microns, as observed.

6.7 Fractal Catalysts

The problem of heterogeneous reactions is of major importance in the chemical industry. The old Wenzel's law [6.88] states that, for heterogeneous reactions, the larger the interface, the faster the reaction. "This is why in industry and in the kitchen one grinds the material in order to speed up the reaction" [6.89].

If a chemical reaction is accelerated on the surface of a catalyst one should use porous catalysts to increase the overall efficiency of the reaction. A number of questions are raised by the dynamics of these complex processes. Very frequently catalyst reactions exhibit noninteger order. Very often the activity of a catalyst follows a power law as a function of the size of the catalyst grain [6.90–94].

Of course catalysts are not necessarily fractal, but the fractal geometry gives a possible hint to the understanding of some part of the catalytic process in specific cases. On the other hand, some very basic growth mechanisms, such as random aggregation or diffusion limited aggregation, build a fractal geometry so that the existence of a fractal aspect in the geometry of irregular materials cannot be considered as exceptional [6.3]. Several chapters of this book discuss the growth of fractal objects.

Several papers have been published on the relation between heterogeneous reactions and fractality (see [6.89–94] and references therein). We present here

a few simple ideas on that matter. In many cases the catalytic activity A of a catalyst particle of size L obeys a power law

$$A \sim L^{d_R}, \tag{6.42}$$

where d_R is called the reaction dimension. Values of d_R ranging from 0.2 to 5.8 have been quoted, but in practice they range from 1 to 3 [6.91,92]. A very simple way to interpret d_R is the notion of active sites. This idea stresses that on a given surface only specific sites are active for catalysis. Suppose that the grain shape is cubic but only the corners of the cube are active for catalysis. Then two grains of different sizes have the same number of active sites and $d_R = 0$.

If the active sites are located on the edges of the cube the activity is proportional to L and $d_R = 1$. If the faces of the cube are active, $d_R = 2$. Experimental values of $d_R < 2$ may indicate that only a fractal subset of the surface is active. Experimental values of $d_R > 2$ may indicate that the catalyst itself has a fractal geometry.

If all sites are active then the activity is proportional to the mass, $A \sim L^{d_f}$ and $d_f = d_R$. These ideas apply if the reactants are present evenly on the catalytic sites, *i.e.*, if the diffusion of reacting species from the source of reactant to the active surface is infinitely fast.

This may not be true and there are many situations where the diffusion of reactants to the active surface (or its active sites) is too slow and so controls the reaction kinetics. Such a process is called an Eley-Rideal mechanism. A third situation exists where the two reactants are on the surface and have to meet after diffusion onto the surface to react. This last mechanism is called the Langmuir-Hinshelwood mechanism. It has specific properties on fractal catalysts. For example, segregation of reactants may appear. This is discussed in [6.89].

Our purpose here is only to show that the results we have described for diffusion to membranes can be transposed to the case of the Eley-Rideal mechanism for heterogeneous catalysis [6.95]. Consider for instance a gas–solid catalysis in the simple case of the reaction

$$A + B \rightarrow AB. \tag{6.43}$$

Normally in a homogeneous phase the reaction rate is

$$\frac{d[AB]}{dt} = K[A][B]. \tag{6.44}$$

In such a case the reaction rate is directly proportional to the first power of the concentration (or pressure) of A and B. The sum of these exponents is 2 and the reaction is said to be second order. It is observed that a large number of heterogeneous reactions follow fractional-order kinetics under different experimental conditions. We show here that the above diffusion scheme gives

rise to that result. Let us consider a case where the efficient reaction process takes place on the surface after adsorption of B atoms. The first step for the reaction is then

$$B_{\text{gas}} \rightarrow B_{\text{ads}}, \tag{6.45}$$

from which the reaction

$$A_{\text{gas}} + B_{\text{ads}} \rightarrow AB_{\text{gas}} \tag{6.46}$$

follows. If the chemical reaction is slow, as in the case of a poor catalyst, the diffusion from the exterior to the walls of the catalyst is accomplished by a small concentration gradient, and the concentration throughout is nearly the same as the external concentration. Fast reactions, however, may take place in the pores very near the exterior, and the internal pore surfaces contribute little. If the activity of the entire surface of the catalyst is compared (if diffusion were infinitely rapid), it is usual for the effectiveness of a poor catalyst to be high and that of an excellent catalyst to be low. Diffusion into the pores involves a decrease in the concentration of the diffusing reactants, and the concentration effective in promoting the chemical reaction at the active sites is everywhere less than if diffusion were not involved. The catalyst, therefore, is less effective than if all the surface were in contact with the reactants at the concentrations maintained in the external or ambient fluid. This loss of catalyst effectiveness due to diffusion is the subject of very many publications.

In general, diffusion within the pores may be ordinary molecular diffusion, Knudsen diffusion, surface diffusion, or a combination of all three. We restrict ourselves here to the consideration of molecular diffusion and we discuss in some detail the equations which describe the population of adsorbed B atoms $[B_{\text{ads}}]$. Without chemical reaction the surface concentration varies by adsorption of molecules from the gas and desorption from the surface, and the rate of absorption is equal to the net flux

$$\frac{d[B_{\text{ads}}]}{dt} = \Phi_n(B) = W_A[B_{\text{gas}}] - W_D[B_{\text{ads}}], \tag{6.47}$$

where $[B_{\text{gas}}]$ is the local partial concentration or partial pressure near the surface and W_A and W_D are the probability per unit time for adsorption and desorption. In the case where reaction (6.46) takes place there is an additional decrease due to the reaction rate proportional to [A] and to $[B_{\text{ads}}]$. Consequently

$$\frac{d[B_{\text{ads}}]}{dt} = W_A[B_{\text{gas}}] - W_D[B_{\text{ads}}] - K_S[A][B_{\text{ads}}], \tag{6.48}$$

where K_S is the reaction coefficient. The steady-state local concentration on the surface is

$$[B_{\text{ads}}] = \frac{W_A[B_{\text{gas}}]}{W_D + K_S[A]}. \tag{6.49}$$

The net flux (6.47) to the surface is simply

$$\Phi_n(B) = \frac{W_A K_S[A][B_{\text{gas}}]}{W_D + K_S[A]}. \tag{6.50}$$

This equation is analogous to (6.36) if we replace W by $W_A K_S[A]/(W_D + K_S[A])$. The catalytic problem is then exactly identical to the membrane problem with the same geometry. A self-affine Sierpinski geometry could be a model for a porous catalyst with hierarchical pore structure on which the reactants are kept at a constant concentration at the entry of the pores. One can then use relation (6.16) or its equivalent for diffusion, which is $Y_p \sim a_0^{(2-\eta)} L^{(2\eta-1)} D^{(1-\eta)} W^{\eta}$. If a given partial pressure $[B]_{\text{ext}}$ of B exists outside the porous system, the net production of AB is the total flux

$$\frac{d[AB]}{dt} \sim a_0^{(2-\eta)} L^{(2\eta-1)} D^{1-\eta} \left(\frac{W_A K_S[A]}{W_D + K_S[A]} \right)^{\eta} [B]_{\text{ext}}. \tag{6.51a}$$

Note that this *"fractal"* speed of reaction is not a linear function of the microscopic sticking probability W_A. Note also that D is the diffusion coefficient of B in A. If B is diluted in A, D is for normal pressures inversely proportional to the concentration or pressure of A. Finally, the rate of reaction will be proportional to

$$\frac{d[AB]}{dt} \sim a_0^{(2-\eta)} L^{(2\eta-1)} [A]^{1-\eta} \left(\frac{W_A K_S[A]}{W_D + K_S[A]} \right)^{\eta} [B]_{\text{ext}}. \tag{6.51b}$$

We have thus presented a model of a catalytic reaction on a fractal surface with a noninteger reaction rate. If $W_D \ll K_S[A]$ (high pressure) the reaction order is η. If $W_D \gg K_S[A]$ (low pressure) the reaction order is 2η. The speed of reaction is a noninteger power-law function of the parameters L and a_0 which describe the macroscopic sizes of the catalyst grain. Although the modified Sierpinski geometry is artificial, it brings to light the idea that reaction order and reaction dimension could be related through simple relations in specific cases.

For a self-similar catalyst one would also find a noninteger order of reaction but the reaction dimension will be equal to 2 from (6.39). For reactions and transport on fractals, see also Chap. 3.

6.8 Summary

This chapter has briefly presented what was known at the end of 1994 about two different but partially related problems: the relation between fractality and the response of irregular electrodes, and the general question of the response of irregular interfaces to Laplacian fields. As these problems have been the subject of several conflicting (or apparently conflicting) results it seems useful to discuss the actual situation.

Let us first consider this situation from the point of view of electrochemistry. The first problem itself can be considered in two ways: First, do fractal electrodes exhibit CPA behavior and how? As we have seen, fractality will generally lead to CPA and the answer to the first part is "yes" and this can be considered as sufficiently documented.

The second, different way is to ask: to what extent can experimental CPA behavior of rough or irregular electrodes be related to fractality? The answer to this question depends on the system. As we have mentioned, a suitable distribution of microscopic parameters could also explain (and contribute to) CPA. In a discussion of porous platinum electrodes, T. Pajkossy has shown that in this specific case microscopic effects are really the source of CPA behavior. Generally speaking, there exist two main objections to fractality as a general explanation for CPA:

1. Fractality leads to Cole-Davidson [6.96] behavior (of the form $Y(\omega) \sim (1+j\gamma\omega\tau)^{\eta}$ as indicated from relation (6.25a)), whereas experimental CPA are often of the Cole-Cole form $Y(\omega) \sim 1 + (j\gamma\omega\tau)^{\eta}$.
2. The frequency range of experimental CPA is often very large, exceeding the range $(L/\ell)^{(d_f-1)}$ that one can expect.

Also, fractal CPA can hold only for objects in which the length $|\Lambda(\omega)| = 1/\rho\gamma\omega$ is larger than the smaller cut-off and smaller than the perimeter. This condition will not be met for rough electrodes (with irregularities in the 10 micron range) in concentrated liquid electrolytes. In contrast, this condition is met for larger electrodes with irregularities on the *mm* or *cm* range or in solid electrolytes (where ρ is smaller).

The conclusion is that geometrical fractality although leading to CPA cannot be used exclusively as the "general" explanation for experimental CPA without checking for the above physical conditions. One should also recall that there exist several electrochemical regimes (diffusion + faradaic or diffusion + resistive as discussed in [6.55] for Sierpinski electrodes) for which no general prediction exists for self-similar electrodes. Also, in the real world both microscopic and geometrical macroscopic effects will probably exist simultaneously. (This was the case in the experiments described in [6.74,76].) For this very reason, exponents alone are not sufficient to ascertain a fractal model. One should check the compatibly of the measurements with relations (6.26–28).

Even more important for the future are the simple results that we have obtained on the general question of the response of irregular interfaces to Laplacian fields. There are three main results:

1. It is possible to find the (linear) response of an irregular interface from its image through an appropriate coarse-graining process.
2. It is a reasonable approximation to consider that there exists a homogeneously active zone and a totally passive zone [6.69,83,84]. In this simplifying approximation it is possible to deal simply with nonlinear responses [6.69].
3. The semiquantitative agreement between the anatomical and physiological data and the expressions that we predict for the "best possible acinus" seems to indicate that the design for the oxygen exchanger in the lung of several animals is optimized. The statement that for the optimized situation the value of the classical admittance of the fractal membrane is equal to the access admittance is very simple. It may thus apply to many situations which are not "simply" fractal.

This brings out the idea of a "perfect exchanger" or "smart filter". One should note that the lung is a simple gas exchanger in the sense that only two gases are exchanged, oxygen and carbon dioxide. (They have approximately the same A.) If one considers the transfer of several species with very different transport parameters, the simultaneous optimization of the transfer should imply that different As should correspond to the same morphology. This cannot be realized by an homogeneous membrane. An optimized fractal multi-species filter or exchanger membrane system could nevertheless be realized by a suitable distribution of specific pores (permeable to specific species) on the membrane. In that sense it is possible that the micro-geometry of the distribution of specific cells (or of cells with active transfer) in inhomogeneous membranes permits the optimization of the transfer of very different species in the same organ. These notions could possibly lead to a better understanding of the morphology and physiology of complex exchangers or filters such as the kidney.

References

6.1 B.B. Mandelbrot: *The Fractal Geometry of Nature* (Freeman, San Francisco 1982)
6.2 J. Feder: *Fractals* (Plenum, New York 1988)
6.3 B. Sapoval: *Fractals* (Aditech, Paris 1990)
6.4 M. Rodriguez, S. Bur, A. Favre, E.R. Weibel: Am. J. Anat. **180**, 143 (1987)
6.5 B. Haeffli-Bleuer, E.R. Weibel: Anat. Record **220**, 401 (1988)
6.6 E.R. Weibel, in: *Respiratory Physiology, an Analytical Approach*, ed. by H.K. Chang, M. Paiva (Dekker, Basel 1989), p. 1
6.7 E.R. Weibel: in *Fractals in Biology and Medicine*, ed. by T.F. Nonnenmacher, G.A. Losa and E.R. Hulin (Birkhäuser, Basel, 1994), p.68

6.8 F. Hallé, R.A.A. Oldeman, P.B. Tomlinson: *Tropical Trees and Forests* (Springer, New York 1978)
6.9 S.W. Benson: *The Foundation of Chemical Kinetics* (McGraw-Hill, New York 1960); A.W. Adamson: *Physical Chemistry of Surfaces* (Wiley, New York 1982)
6.10 R. Ball, M. Blunt: J. Phys. A: Math. Gen. **21**, 197 (1988)
6.11 J.B. Bates, Y.T. Chu: Solid State Ionics **28-30**, 1388 (1988)
6.12 J.B. Bates, J.C. Wang, Y.T. Chu: Solid State Ionics **18/19**, 1045 (1986)
6.13 J.B. Bates, Y.T. Chu, W.T. Stribling: Phys. Rev. Lett. **60**, 7, 627 (1988)
6.14 R. Blender, W. Dieterich, T. Kirchhoff, B. Sapoval: J. Phys. A: Math. Gen. **23**, 1225 (1990)
6.15 M. Blunt: J. Phys. A **22**, 1179 (1989)
6.16 E. Chassaing, B. Sapoval, G. Daccord, R. Lenormand: J. Electroanal. Chem. **279**, 67 (1990)
6.17 Y.T. Chu: Solid State Ionics **23**, 253 (1987)
6.18 Y.T. Chu: Solid State Ionics **26**, 299 (1988)
6.19 L. Fruchter, G. Crepy, A. Le Méhauté: J. Power Sources **18**, 51 (1986)
6.20 W. Geertsma, J.E. Gols, L. Pietronero: Physica A **158**, 691 (1989)
6.21 W. Geertsma, J.E. Gols: J. Phys. C: Condens. Matter **1**, 4469 (1989)
6.22 P.G. de Gennes: C.R. Acad. Sci. (Paris) **295**, 1061 (1982)
6.23 L.J. Gray, S.H. Liu, T. Kaplan, in: *Scaling Phenomena in Disordered Systems*, ed. by R. Pynn, A. Skjeltorp (Plenum, New York 1985)
6.24 T.C. Halsey: Phys. Rev. A **35**, 3512 (1987)
6.25 T.C. Halsey: Phys. Rev. A **36**, 5877 (1987)
6.26 R.M. Hill, L.A. Dissado: Solid State Ionics **26**, 295 (1988)
6.27 T. Kaplan, L.J. Gray: Phys. Rev. B **32**, 11, 7360 (1985)
6.28 T. Kaplan, S.H. Liu, L.J. Gray: Phys. Rev. B **34**, 4870 (1986)
6.29 T. Kaplan, L.J. Gray, S.H. Liu: Phys. Rev. B **35**, 5379 (1987)
6.30 M. Keddam, H. Takenouti: C.R. Acad. Sci. (Paris) **302** Sér. II, 281 (1986)
6.31 M. Keddam, H. Takenouti: Electrochim. Acta **33**, 445 (1988) and 40th I.S.E. Meeting, Kyoto, Japan (1989) Ext. Abst. d2, 1183
6.32 M. Keddam, H. Takenouti, in: *Fractal Aspects of Materials*, ed. by R.B. Leibowitz, B.B. Mandelbrot, D.E. Passoja (Material Research Society, Pittsburgh 1985), p. 89
6.33 A. Le Méhauté: Electrochim. Acta **34**, 4, 591 (1989)
6.34 A. Le Méhauté, G. Crépy: Solid State Ionics **9/10**, 17 (1983)
6.35 A. Le Méhauté, G. Crepy, A. Hurd, D. Schaefer, J. Wilcoxon, S. Spooner: C.R. Acad. Sc. (Paris) **304**, 491 (1987)
6.36 A. Le Méhauté, A. Dugast: J. Power Sources **9**, 35 (1983)
6.37 R. de Levie: J. Electroanal. Chem. **261**, 1 (1989)
6.38 S.H. Liu: Phys. Rev. Lett. **55**, 529 (1985)
6.39 S.H. Liu, T. Kaplan, L.J. Gray, in: *Fractals in Physics*, ed by L. Pietronero, E. Tossati (North-Holland, Amsterdam 1986), p. 383
6.40 S.H. Liu, T. Kaplan, L.J. Gray: Solid State Ionics **18/19**, 65 (1986)
6.41 E.T. McAdams: Surface Topography **2**, 107 (1989)
6.42 A. Maritan, A.L. Stella, F. Toigo: Phys. Rev. B **40**, 9267 (1989)
6.43 A.M. Marvin, F. Toigo, A. Maritan: Surf. Sci. **211/212**, 422 (1989)
6.44 W.H. Mulder, J. H. Sluyters: Electrochim. Acta **33**, 303 (1988)
6.45 L. Nyikos, T. Pajkossy: Electrochim. Acta **30**, 1533 (1985)
6.46 L. Nyikos, T. Pajkossy: Electrochim. Acta **31**, 1347 (1986)
6.47 L. Nyikos, T. Pajkossy: Electrochim. Acta **35**, 1567 (1990)
6.48 T. Pajkossy, L. Nyikos: J. Electrochem. Soc. **133**, 2061 (1986)
6.49 T. Pajkossy, L. Nyikos: Electrochim. Acta **34**, 171 (1989)
6.50 T. Pajkossy, L. Nyikos: Electrochim. Acta **34**, 181 (1989)
6.51 T. Pajkossy: J. Electroanal. Chem. **300**, 1 (1991)
6.52 B. Sapoval: Solid State Ionics **23**, 253 (1987)
6.53 B. Sapoval: *Fractal Aspects of Materials, Disordered Systems* (Materials Research Society, Pittsburgh 1987), p. 66

6.54 B. Sapoval, J.-N. Chazalviel, J. Peyrière: Solid State Ionics **28-30**, 1441 (1988)
6.55 B. Sapoval, J.-N. Chazalviel, J. Peyriere: Phys. Rev. A **38**, 5867 (1988) and references therein
6.56 B. Sapoval: Acta Stereologica **6/III**, 785 (1987)
6.57 B. Sapoval, E. Chassaing: Physica A **157**, 610 (1989)
6.58 J.C. Wang, J.B. Bates: Solid State Ionics **18/19**, 224 (1986)
6.59 J.C. Wang: J. Electrochem. Soc, **134**, 1915 (1987)
6.60 J.C. Wang: Solid State Ionics **28-30**, 143 (1988)
6.61 W. Scheider: J. Phys. Chem. **79**, 127 (1975) and references therein
6.62 R. de Levie, Electrochim. Acta **8**, 751 (1953); **10**, 113 (1965)
6.63 R.D. Armstrong, R.A. Burnham: J. Electroanal. Chem. **72**, 257 (1976)
6.64 P.H. Bottelberghs, in: *Solid Electrolytes*, ed. by P. Hagenmuller, W. Van Gool (Academic, New York 1978)
6.65 P.H. Bottelberghs, H. Erkelens, L. Louwerse, G.H.J. Broers: J. Appl. Electrochem. **5**, 165 (1975); P.H. Bottelberghs, G.H.J. Broers: J. Electroanal. Chem. **67**, 155 (1976)
6.66 J.R. Macdonald: J. Appl. Phys. **58**, 1955 (1985); J. Appl. Phys. **62**, R51 (1987) and references therein
6.67 T. Pajkossy: J. Electroanal. Chem. **364**, 111 (1994)
6.68 C. Tricot: Phys. Lett. A**114**, 430 (1986)
6.69 B. Sapoval: Solid State Ionics **75**, 269 (1995)
6.70 B. Sapoval: J. Electrochem. Soc. **137**, 144C (1990); Extended Abstract, Spring Meeting of the Electrochemical Society, Pennington 1990, p.772
6.71 P. Meakin, B. Sapoval: Phys. Rev. A **43**, 2893 (1991)
6.72 N.G. Makarov: Proc. London Math. Soc. **51**, 369 (1985)
6.73 R.P. Wool, J.M. Long: Macromolecules: **26**, 5227 (1993); R.P. Wool: *Structure and Strength of Polymer Interfaces* (Hanser publ. 1994). In these references the number S is used to describe the relative irregularity of fractal "diffusion front"
6.74 B. Sapoval, R. Gutfraind, P. Meakin, M. Keddam, H. Takenouti: Phys. Rev. E **48**, 3333 (1993)
6.75 W.H. Mulder, J.H. Sluyters, T. Pajkossy and L. Nyikos: J. Electroanal. Chem. **285**, 103 (1990)
6.76 E. Chassaing, B. Sapoval: J. Electrochem. Soc. **141**, 2711 (1994)
6.77 G. Daccord, R. Lenormand: Nature (London) **325**, 41 (1987)
6.78 T.C Halsey, M. Liebig: Europhys. Lett. 14, 815 (1991) and Phys. Rev. A **43**, 7087 (1991)
6.79 R.C. Ball: in *Surface Disordering, Growth, Roughening and Phase Transitions*, ed. by R. Julien, P. Meakin, D. Wolf (Nova Science Publisher, 1993), p.277
6.80 T.C Halsey and M. Liebig: Annals Phys. **219**, 109 (1992)
6.81 M. Liebig, T.C Halsey: J. Electroanal. Chem. **358**, 77 (1993)
6.82 H. Ruiz-Estrada, R. Blender and W. Dieterich: to be published in J. Phys.: Condens. Matter (1994)
6.83 B. Sapoval: in *Surface Disordering, Growth, Roughening and Phase Transitions*, ed. by R. Julien, P. Meakin, D. Wolf (Nova Science Publisher, 1993), p.285
6.84 R. Gutfraind, B. Sapoval: J. Physique I **3** 1801 (1993)
6.85 B. Sapoval in *Fractals in Biology and Medicine*, ed. by T.F. Nonnenmacher, G.A. Losa and E.R. Hulin (Birkhäuser, Basel, 1994), p.241
6.86 R. Gutfraind, B. Sapoval: in *Fractals in Biology and Medicine*, ed. by T.F. Nonnenmacher, G.A. Losa and E.R. Hulin (Birkhäuser, Basel, 1994), p.251
6.87 A. Beaumont, P. Cassier: *Biologie Animale* (Dunod Université, Paris, 1978), p.443
6.88 C.F. Wenzel: *Lehre von der Verwandtschaft der Körper* (Dresden, 1777)
6.89 R. Kopelman, in: *The Fractal Approach to Heterogeneous Chemistry*, ed. by D. Avnir (Wiley, New York 1989), p. 295 and references therein
6.90 P. Pfeiffer, D. Avnir, D. Farin: J. Stat. Phys. **36**, 199 (1984)
6.91 D. Farin, D. Avnir: J. Am. Chem. Soc. **110**, 2039 (1988)
6.92 D. Farin, D. Avnir: J. Phys. Chem. **91**, 5517 (1987)
6.93 D. Farin, D. Avnir, in: *The Fractal Approach to Heterogeneous Chemistry*, ed. by D. Avnir (Wiley, New York 1989), p. 271 and references therein

6.94 D. Avnir, R. Gutfraind and D. Farin: in *Fractals in Science*, ed. by A. Bunde and S. Havlin (Springer-Verlag, 1994), chap. 8
6.95 B. Sapoval: C.R. Acad. Sci. (Paris) **312**, Sér. II, 599 (1991)
6.96 D.W. Davidson and R.H. Cole: J. Chem. Phys. **19**, 1484 (1951)